LWT - Food Science and Technology 181 (2023) 114738

Contents lists available at ScienceDirect

LWT

journal homepage: www.elsevier.com/locate/lwt

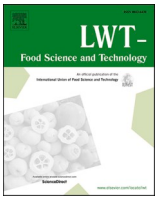

Development of propolis extract-loaded nanoparticles with chitosan and hyaluronic acid for improving solubility and stability

Do Hee Kim, Eun Woo Jeong, Youjin Baek, Hyeon Gyu Lee *

Department of Food and Nutrition, Hanyang University, 222 Wangsimni-ro, Seongdong-gu, Seoul, 04763, South Korea

ARTICLE INFO

Keywords:
Propolis extract
Encapsulation
Hyaluronic acid
Solubility
Stability

ABSTRACT

Propolis extract (PE) is a natural polyphenol with various biological activities; however, its application is limited due to low solubility and instability. To overcome these drawbacks, we encapsulated PE in nanoparticles (PE-loaded nanoparticles, PE-NP) using chitosan (CS) and hyaluronic acid (HA) as wall materials. We examined the physicochemical characteristics (size, polydispersity index, zeta potential, and entrapment efficiency) of PE-NP prepared with the various ratios of CS to HA and core to the wall material, and confirmed the optimal ratio for the formulation of PE-NP as 4:7 and 1:2, respectively. In addition, PE-NP significantly increased the solubility of PE by 2.43-fold compared to that of free PE ($p < 0.05$). Moreover, the retention rate of total flavonoid content (TFC) in PE-NP was significantly higher than that in free PE after the heat treatment (90 °C) for 24 h ($p < 0.05$). Furthermore, PE-NP showed significantly higher retention rates of TFC and DPPH radical scavenging effects than free PE after storage for 4 weeks at 30 and 50 °C ($p < 0.05$). In conclusion, these findings suggest that PE-NP may be a promising approach to enhance the solubility and stability of PE and could provide helpful information for expanding the application of PE.

1. Introduction

Propolis is a natural phytochemical compound, a mixture of plant resins and the salivary secretion of bees (Santos et al., 2020). Propolis is composed of 50% resin, 30% wax and fatty acids, 10% essential oils, and 5% pollen (Boisard et al., 2015). Propolis extract (PE) is obtained after the wax removal, followed by solvent or supercritical extraction. PE contains high levels of flavonoids such as quercetin, chrysin, galangin, and pinocembrin (Iadnut et al., 2019). In addition, several biological activities of PE, including antioxidant, anti-inflammatory, antimicrobial, antitumor, and antiviral activities have been reported owing to the abundance of flavonoids (Anjum et al., 2019). Despite its health-promoting effects, the application of PE has been limited owing to its low water solubility and instability (do Nascimento et al., 2022; Jansen-Alves et al., 2019). To overcome these drawbacks, previous studies have attempted to encapsulate PE using various carriers such as particles, liposomes, emulsions, and cyclodextrins (Zhang et al., 2019; Ramli, Ali, Hamzah, & Yatim, 2021; Seibert et al., 2019; Kalogeropoulos et al., 2009).

Encapsulation is a promising technique because it can increase solubility and bioavailability and prevent degradation by heat, oxidation, and UV (Fang & Bhandari, 2010). Among the various encapsulation methods, nanoparticles (NP) have advantages such as long shelf life and high entrapment efficiency. Moreover, NP protect core materials from degradation or deactivation before reaching the target site (Anselmo & Mitragotri, 2014). Furthermore, they can be manufactured with natural, non-toxic, biocompatible, and biodegradable materials and are regarded as safe (Wu, Yang, Wang, Hu, & Fu, 2005).

Chitosan (CS) is a widely used cationic biopolymer, produced by the deacetylation of chitin present in crab or shrimp shells. It can be used to fabricate NP through electrostatic interactions with anionic biopolymers, such as hyaluronic acid (HA), gum arabic, and dextran sulfate. HA is an anionic polysaccharide that is widely distributed throughout the human body, particularly in the skin, connective tissue, intestine, and eyes (Oyarzun-Ampuero, Brea, Loza, Torres, & Alonso, 2009). HA exhibits a strong affinity for CD44, a cell surface protein that is overexpressed in many types of cancer cells and cancer stem cells (Platt & Szoka, 2008). The utilization of NP formulated with HA has been mainly focused on the pharmaceutical industry. Our previous study suggested the possibility of HA as a promising wall material with CS as an oral delivery system in the food industry, with high mucoadhesive properties, cell permeability, and antioxidant activity compared to those of

* Corresponding author.
E-mail address: hyeonlee@hanyang.ac.kr (H.G. Lee).

https://doi.org/10.1016/j.lwt.2023.114738
Received 16 January 2023; Received in revised form 19 March 2023; Accepted 5 April 2023
Available online 10 April 2023

other anionic biopolymers (Kim, Lee, & Lee, 2021). However, no study has investigated the optimal preparation conditions for PE-loaded nanoparticles (PE-NP) under both CS/HA and core/wall ratios. Furthermore, to the best of our knowledge, none of the studies have attempted to enhance the solubility and thermal and storage stabilities of PE by NP with CS and HA.

The aim of this study was to investigate the optimal CS/HA and core/wall ratios for the formulation of PE-NP, and the effects of PE-NP on solubility and stability. To this end, PE-NP were prepared by ionic gelation between CS and HA by controlling the CS/HA and core/wall material ratios. Then, their physicochemical properties, such as size, polydispersity index (PDI), zeta potential, and entrapment efficiency, were measured. More importantly, the efficacy of HA for the encapsulation of PE in terms of solubility and thermal and storage stabilities was revealed in our study.

2. Materials and methods

2.1. Materials

PE was donated by Neo Cremar Co. Ltd (Sungnam, Korea). Low-molecular-weight chitosan, L-α-phosphatidylcholine, aluminum chloride hexahydrate, 6-hydroxy-2,5,7,8-tetramethylchroman-2-carboxylic acid (Trolox), 2,2′-azino-bis(3-ethylbenzothiazoline-6-sulfonic acid) diammonium salt (ABTS), potassium persulfate, sodium phosphate dibasic, fluorescein isothiocyanate isomer, and 2′-azobis(2-methylpropionamidine) dihydrochloride (AAPH) were purchased from Sigma-Aldrich Chemical Co. (St. Louis, MO, USA). Hyaluronic acid and cholesterol were obtained from Bioland (Cheonan, Korea) and Yakuri Pure Chemicals Co. (Kyoto, Japan), respectively. 2,2-Diphenyl-1-picrylhydrazyl (DPPH) was purchased from Alfa Aesar (Ward Hill, MA, USA). Quercetin dihydrate was purchased from the Shanghai Aladdin Biochemical Technology Co. (Shanghai, China). Trehalose dihydrate and potassium phosphate monobasic were purchased from Tokyo Chemical Industry (TCI) (Tokyo, Japan) and Daejung Chemical and Metals Co. (Siheung, Korea), respectively. All chemicals used in this study were of analytical grade.

2.2. Preparation of PE-loaded nanoparticles (PE-NP)

PE-NP were prepared by the ionic gelation method, which involved electrostatic interactions between the amino groups of CS and the carboxyl groups of HA (Lu, Zhao, Wang, & Lv, 2011). CS, HA, and PE were completely dissolved in 1 mL/100 mL acetic acid, distilled water, and ethanol, respectively. Under magnetic stirring (1000 rpm) at room temperature, 1 mL of PE was added to 7 mL of the CS solution at a flow rate of 1.0 mL/min and stirred for 10 min. Then, 2 mL of the HA solution was added to the 8 mLCS solution containing PE and stirred for 20 min. The mass ratios of CS to HA were adjusted to 4:5, 4:6, 4:7, 4:8, and 4:9 (w/w) and the final concentration of PE was 0.4 mg/mL. Moreover, the mass ratios of the core (PE) to the wall materials (CS/HA) were set to 1:2, 1:3, and 1:4 (w/w).

2.3. Physicochemical properties of PE-NP

The particle size, PDI, and zeta potential of PE-NP were investigated using the dynamic light scattering method with a Malvern Zetasizer Nano ZS (Malvern Instruments Ltd., Malvern, UK). The entrapment efficiency of PE-NP was indirectly determined by measuring the TFC entrapped within the PE-NP, as previously described (Zhang et al., 2019). PE-NP were ultracentrifuged at 4,000×*g* for 30 min at 4 °C using a 50 kDa centrifugal filter device (Amicon Ultra-4 Centrifugal Filter, Millipore, Billerica, MA, USA). Free PE was quantified by measuring the TFC of the filtrate. Entrapment efficiency (%) was calculated using the following equation (1):

$$\text{Entrapment efficiency}\ (\%) = \{(\text{total amount of total flavonoid content} - \text{free amount of total flavonoid content})\ /\ \text{total amount of total flavonoid content}\} \times 100 \quad (1)$$

The TFC was measured using a modified method of Chang, Yang, Wen, & Chern, 2002. Briefly, each sample was mixed with the same volume of 20 mg/mL solution of aluminum chloride. The mixture was then vortexed and incubated at 25 °C for 10 min. The absorbance was read at 415 nm on a Synergy HT Multi-microplate reader (Bio-Tek Instrument Inc., Winooski, VT, USA). TFC was expressed as milligrams of quercetin equivalent (QUE) per gram of the sample (mg QUE/g).

2.4. Morphological characterization

The shape and surface morphology of propolis extract-unloaded nanoparticles (BLK-NP) and PE-NP were investigated by scanning electron microscopy (SEM) (Verios G4UC, FEI, Hillsboro, OR, USA) (Kaushik and Roos. 2007). Freeze-dried samples were mounted onto carbon tape and coated with platinum. They were then analyzed at an acceleration voltage of 5 kV.

2.5. Solubility of PE-NP

The effect of PE-NP on solubility was evaluated as previously described (Lee, Kim, & Lee, 2017). The solubilities of both free PE and PE-NP were analyzed after lyophilization. As a cryoprotectant, 50 mg/mL trehalose was added to the PE-NP suspension and freeze-dried for 48 h. Lyophilized PE-NP were suspended in the same volume of distilled water before lyophilization and stirred for 10 min. They were then centrifuged at 3,000×*g* for 10 min. The supernatant was filtered through a membrane filter with a pore size of 0.45 μm to remove the remaining insoluble PE. To rupture PE-NP, 0.5 mL of the sample and 0.5 mL of acetonitrile were mixed and vortexed for 30 s as previously described (Smits, Smits, & Vromans, 2013). The mixture was incubated for 10 min at 25 °C. The completely dissolved PE was quantified by measuring TFC, as previously mentioned in Section 2.3.

2.6. Stability of PE-NP

2.6.1. Thermal stability

Free PE and PE-NP were incubated at 90 °C in the dark for 24 h. The retention rates of TFC were measured after 2, 4, 12, and 24 h of heat treatment to investigate the thermal stability, following the procedure described in Section 2.4 (Muhammad et al., 2020). Retention rate (%) was calculated using the following equation (2):

$$\text{Retention rate}\ (\%) = (\text{residual TFC after storage}\ /\ \text{initial TFC}) \times 100 \quad (2)$$

2.6.2. Storage stability

Free PE and PE-NP were stored at 30 and 50 °C in the dark for 4 weeks (Chang, Feng, He, Chen, & Liang, 2020). The retention rates of TFC and DPPH radical scavenging effects were measured every week to investigate storage stability, according to the procedure described in

sections 2.3 and 2.6.1.

The DPPH radical scavenging assay was performed according to the method described by (Bai et al., 2019) with slight modifications. An aliquot of each sample was mixed with the same volume of 0.36 mM DPPH ethanol solution and placed in the dark for 30 min at 25 °C. The samples were then centrifuged at 17,000 rpm for 10 min. The absorbance of the supernatant was measured at 517 nm using a microplate reader. The DPPH radical scavenging activity was calculated using the following equation (3):

$$\text{Entrapment efficiency } (\%) = \{(\text{absorbance of control} - \text{absorbance of sample}) \ / \ \text{absorbance of sample}\} \times 100 \quad (3)$$

2.7. Statistical analysis

All experiments were performed in triplicates. The results are presented as mean ± standard deviation. The results were analyzed using a Student's t-test and one-way analysis of variance, followed by Duncan's multiple range test using SPSS Version 26.0 (SPSS Inc., Chicago, IL, USA). Differences were considered statistically significant at $p < 0.05$.

3. Results and discussion

3.1. Physicochemical properties of PE-NP prepared under various conditions

3.1.1. Effect of CS/HA ratio

The physicochemical properties of PE-NP prepared with the different mass ratios of CS/HA are shown in Fig. 1. The sizes of PE-NP with different CS/HA ratios ranged from 357.5 ± 14.1 nm to 378.3 ± 6.1 nm. The CS/HA ratio did not significantly change the size of PE-NP. Interestingly, as the HA concentration increased, the PDI significantly decreased from 0.424 ± 0.059 to 0.173 ± 0.019 and the zeta potential significantly decreased from 29.6 ± 1.7 to 21.0 ± 0.7 mV ($p < 0.05$). In addition, the entrapment efficiency of PE-NP ranged from 85.8 ± 0.3 to 91.2 ± 0.5%, and the highest entrapment efficiency was obtained with a CS/HA ratio of 4:7.

In this study, the CS/HA ratio did not significantly affect the size of PE-NP; however, they did affect the PDI, zeta potential, and entrapment efficiency of PE-NP. These results are similar to a previous study in which the sizes of pDNA-loaded CS/HA NP (267.7–328.1 nm) did not change significantly regardless of the changes in CS/HA ratio (Oliveira, Bitoque, & Silva, 2014). In addition, the result that PDI significantly increased with increasing CS concentration could be explained by a previous study showing that superfluous CS beyond the optimum level in PE-NP suspension may produce aggregates (Kim, Baek, Yoo, Lee, & Lee, 2022). The PDI values of PE-NP with 4:5 and 4:6 ratios were higher than 0.3, implying heterogeneous dispersion, and these results may be due to CS aggregates (Lee, Kim, & Lee, 2017).

Moreover, the increase in HA concentration resulted in a decrease in zeta potential due to an increase in the degree of neutralization of amino groups, as PE-NP were prepared by ionic gelation between the positively charged amino groups of CS and the negatively charged carboxyl groups of HA (Lu et al., 2011). Furthermore, high entrapment efficiencies (85.8 ± 0.3 to 91.2 ± 0.5%) in PE-NP were obtained in this study compared with those in previous research (Cavalu et al., 2018; Zhang et al., 2018). For instance (Cavalu et al., 2018), reported that the entrapment efficiency of PE-NP prepared with CS and gum arabic reached 71%. The high entrapment efficiency of PE-NP in our study may be due to the hydrophilic property of HA. In addition, HA, a high molecular weight polysaccharide, ~~which~~ may contribute to having a denser structure as a barrier, thereby entrapping PE effectively (Akolade, Oloyede, & Onyenekwe, 2017; Yang et al., 2015). The highest entrapment efficiency (91.2 ± 0.5%) was obtained in PE-NP with a 4:7 ratio because superfluous CS and HA caused aggregates and low stability, decreasing entrapment efficiency. Taken together, these findings indicated that the CS/HA ratio significantly affected the PDI, zeta potential, and entrapment efficiency of PE-NP, but not their size. Based on the above results, a 4:7 CS/HA ratio was confirmed as the optimal ratio for preparing PE-NP and was used in further experiments.

3.1.2. Effect of core/wall ratio

PE-NP were prepared with different mass ratios of core (PE) to wall materials (CS/HA), and their physicochemical properties are shown in Fig. 2. As the concentration of wall material increased from 1:2 to 1:4, the size and PDI significantly increased from 378.3 ± 6.1 to 549.5 ± 30.3 nm and from 0.309 ± 0.018 to 0.495 ± 0.017, respectively ($p < 0.05$); however, there was no significant change in the zeta potential. The entrapment efficiency of PE-NP decreased significantly as the amount of wall material increased ($p < 0.05$).

These findings indicate that the core/wall material ratio has a significant effect on the size, PDI, and entrapment efficiency but not on the zeta potential of PE-NP. These observations are consistent with a previous study which showed that an increase in the concentration of wall material led to an increase in the size and PDI (Yazicioglu, Sahin, & Sumnu, 2015). This phenomenon can be explained by the formation of thick layers and aggregation between small PE-NP as the concentration of the wall material increased. According to a previous study, the excessive wall material content, compared to the core material content, has a remarkable influence on entrapment efficiency, since an amount of wall material above the optimal level would induce aggregation and release of PE (Ghatak & Iyyaswami, 2019). For instance, Shao, Xuan, Wu, & Qu, 2019 reported that the highest entrapment efficiency was obtained at a core/wall ratio of 1:2 among the different ratios (1:1, 1:2, 1:3, and 2:1). A previous study reported that the core/wall ratio had no significant influence on the zeta potential of saffron essential oil-loaded NP (Astutiningsih, Anggrahini, Fitriani, & Supriyadi, 2022). Based on the above results, a core/wall ratio of 1:2 was selected for further studies.

3.2. Morphological characterization

To observe the morphology of BLK-NP and PE-NP prepared under optimal conditions, they were analyzed using SEM. As shown in Fig. 3a and b, both BLK-NP and PE-NP possessed similar glass-like structures. The surfaces of both BLK-NP and PE-NP were smooth and free of cracks (Fig. 3c and d). The morphology of PE-NP was in accordance with a previous report (Chen, Chi, & Xu, 2012). Lemon pomace aqueous extract-loaded NP, developed using maltodextrin and carrageenan, showed broken glass or flake-like structures formed by the dehydration process during freeze-drying (Chen et al., 2012; Kaushik & Roos, 2007). This may be due to the lack of force to break up the frozen suspension into droplets at low temperatures during freeze-drying (Chen et al., 2012). Kaushik & Roos reported that an amorphous structure could protect entrapped PE from harsh environments such as heat, light, and oxygen. Moreover, the existence of cracks on the surface of lyophilized PE-NP may have an adverse effect on redispersibility (Kaushik & Roos, 2007). Thus, our observations suggested a successful encapsulation of

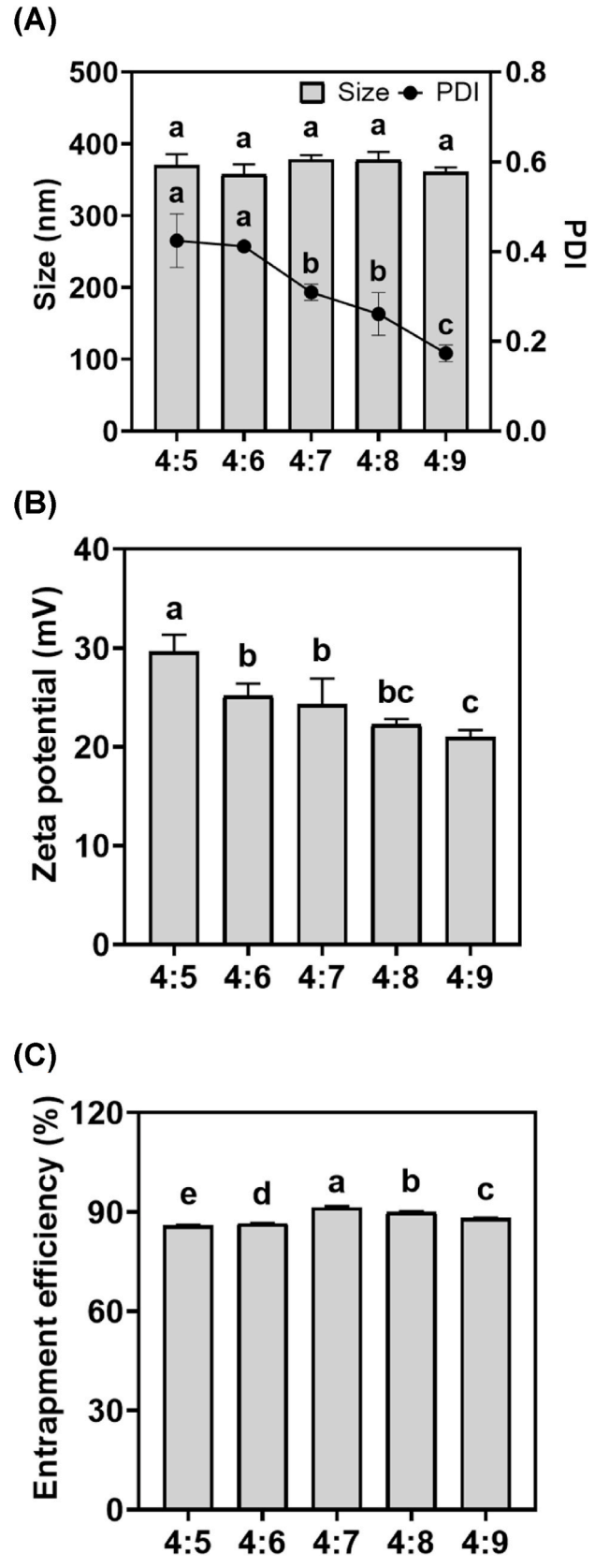

Fig. 1. The effect of the mass ratio of CS to HA on the (a) size and PDI, (b) zeta potential, and (c) entrapment efficiency of PE-NP. CS, chitosan; HA, hyaluronic acid; PE-NP, propolis extract-loaded nanoparticles; PDI, polydispersity index. All data are expressed as mean ± standard deviation. [a–e] The values with different letters are significantly different by Duncan's multiple range test $p < 0.05$.

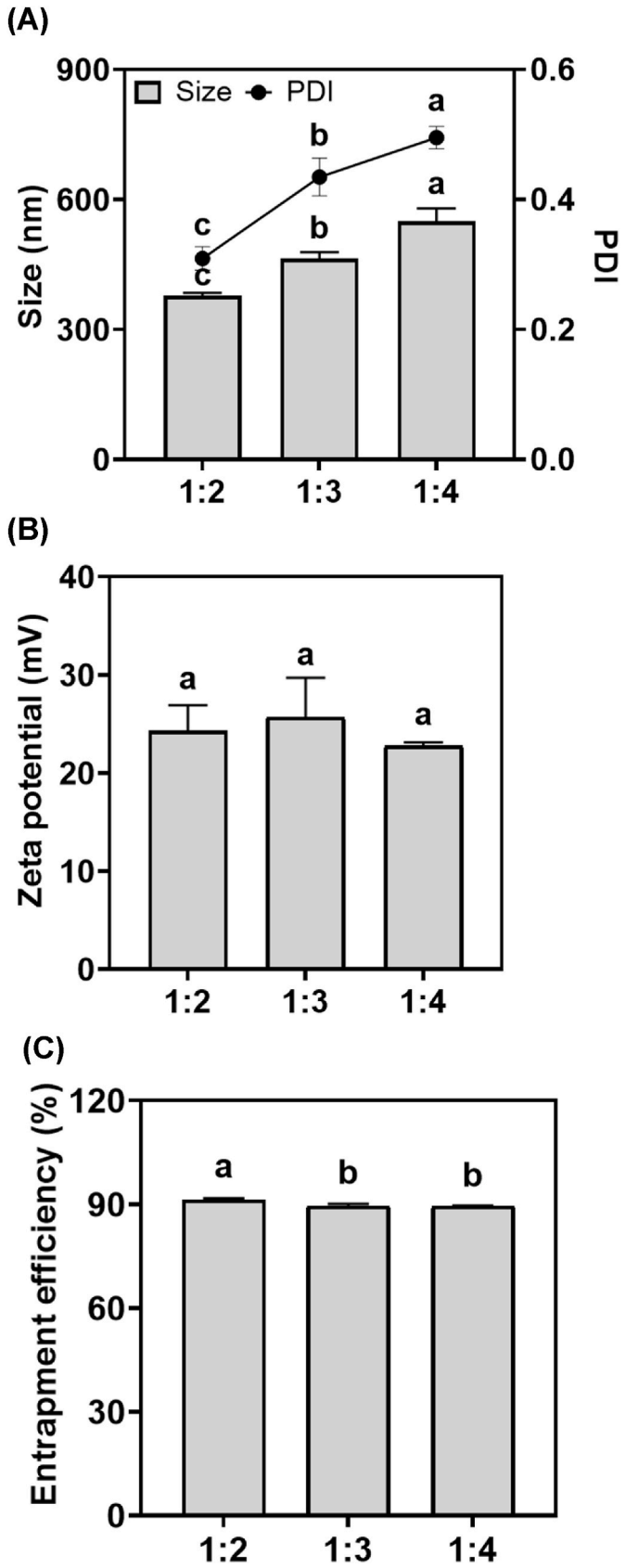

Fig. 2. The effect of the mass ratio of core to wall materials on (a) size and PDI, (b) zeta potential, and (c) entrapment efficiency of PE-NP. PE-NP, propolis extract-loaded nanoparticles; PDI, polydispersity index. All data are expressed as mean ± standard deviation. [a–c] The values with different letters are significantly different by Duncan's multiple range test $p < 0.05$.

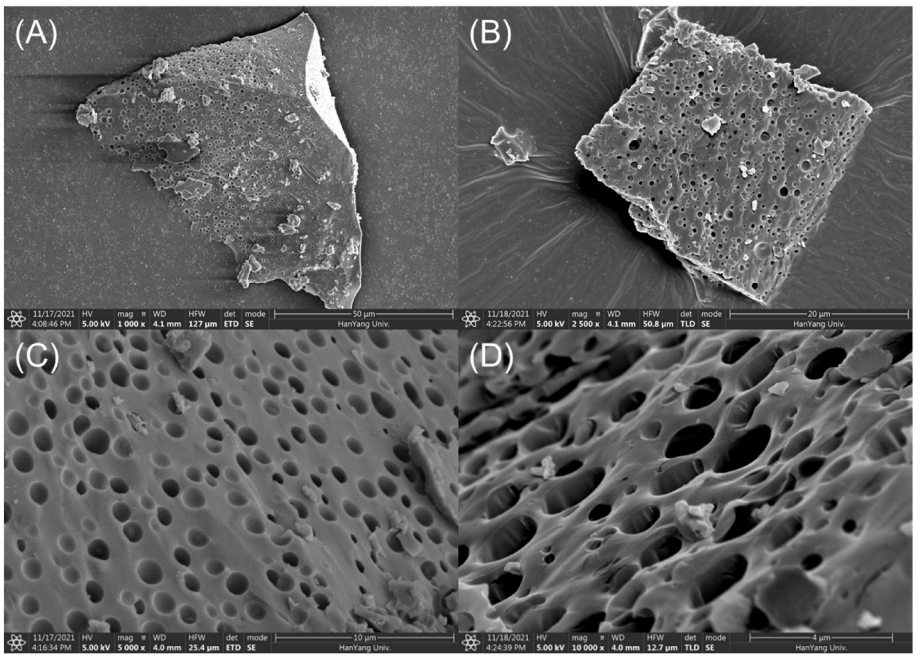

Fig. 3. SEM images of (a) BLK-NP (1,000x magnification), (b) PE-NP (2.500x magnification), (c) BLK-NP surface (5,000x magnification), and (d) PE-NP surface (10,000x magnification). SEM, scanning electron microscopy; BLK-NP, propolis extract-unloaded nanoparticles; PE-NP, propolis extract-loaded nanoparticles.

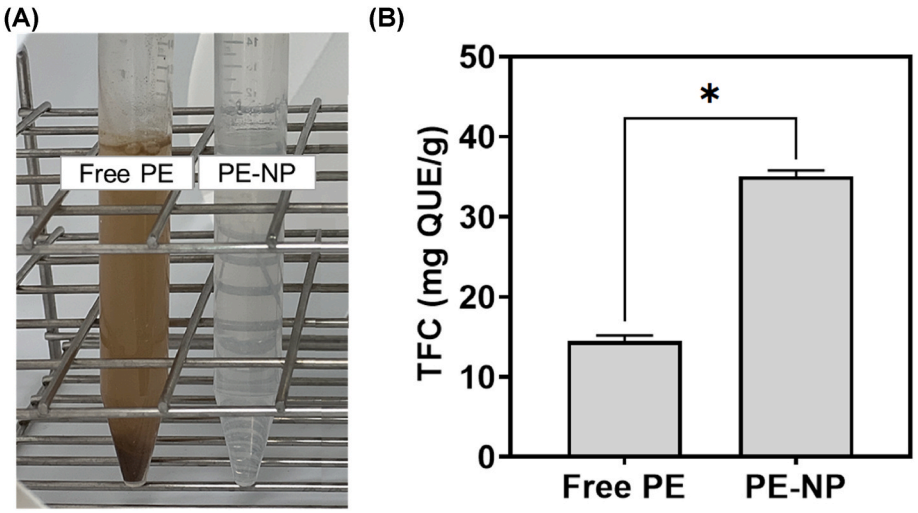

Fig. 4. (a) The appearance of free PE and PE-NP dispersed in distilled water and (b) their solubility, while the PE concentration was fixed at 0.4 mg/mL. PE-NP, propolis extract-loaded nanoparticles. All data are expressed as mean ± standard deviation. *Asterisk indicates a significant difference between the two groups using the Student's t-test at $p < 0.05$.

PE into glass-like structures and the possibility of PE-NP enhancing solubility and stability.

3.3. Solubility of PE-NP

As denoted in Fig. 4a and b, the effect of PE-NP on solubility was investigated. The PE concentrations of both samples were fixed at 0.4 mg/mL. TFC in free PE and PE-NP was 14.43 ± 0.71 and 35.03 ± 0.75 mg QUE/g, respectively, indicating that the solubility of PE-NP remarkably increased by 2.43-fold compared to that of free PE ($p < 0.05$). In addition, PE-NP were thoroughly redispersed in distilled water without agglomeration.

According to previous studies, CS-based NP enhanced the solubility of insoluble materials. For instance, the solubility of coenzyme Q10-loaded NP prepared with CS and two types of anionic biopolymers, sodium triphosphate and dextran sulfate, increased approximately 1.24 times compared to free coenzyme Q10 (Lee, Suh, Kim, & Lee, 2017). Enhanced solubility was also reported by (Jeon, Lee, & Lee, 2016), who demonstrated the efficiency of NP prepared with CS and γ-poly glutamic acid in enhancing the solubility of resveratrol. However, there have been no previous studies on the effect of NP made of CS and HA on the solubility of insoluble substances. The higher solubility of PE-NP compared to that of free PE could be explained by the increased surface area and reduced molecular mobility (Lee, Kim, & Lee, 2017). The larger surface area of PE-NP compared to that of free PE allowed PE to interact with the medium more effectively. In addition, the high mobility of dried extract tends to cause stickiness, caking, and aggregation and impair dispersibility and solubility (Li, Lin, Roos, & Miao, 2019). In contrast, as shown in the 1H NMR spectroscopy of a free insoluble drug and its solid dispersion with HA, encapsulation with HA exhibit a decrease in the

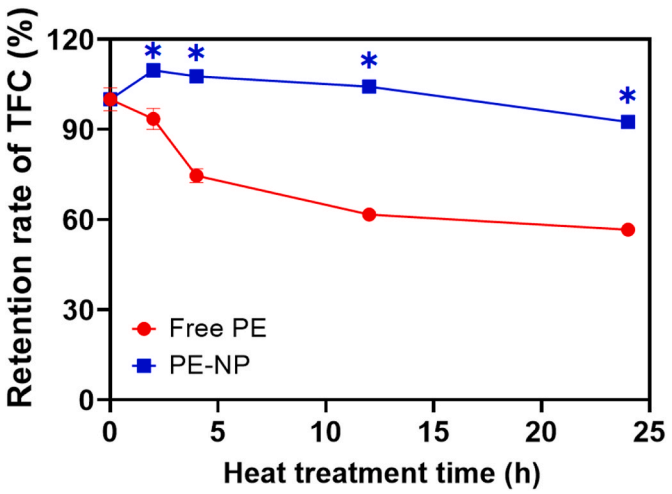

Fig. 5. Thermal stability of free PE and PE-NP under heat treatment at 90 °C for 24 h. PE, propolis extract; PE-NP, propolis extract-loaded nanoparticles. All data are expressed as mean ± standard deviation. *Asterisk indicates a significant difference between the two groups using the Student's t-test at $p < 0.05$.

NMR peak resolution, indicating a decrease in molecular mobility and an increase in solubility (Wei et al., 2022). Another possible explanation for the high solubility is the hydrophilic property of HA (Choh, Cross, & Wang, 2011). Similarly, the solubility of decoquinate-loaded solid dispersion was higher than that of free decoquinate, owing to the interaction between hydrophilic HA and hydrophobic decoquinate (Wei et al., 2022). This is the first study to show that NP with CS and HA significantly enhanced the solubility of PE. Taken together, PE-NP have a remarkable potential to enhance the solubility of PE.

3.4. Stability of the PE-NP

3.4.1. Thermal stability of the PE-NP

The thermal stability of the free PE and PE-NP was investigated by measuring the residual TFC after heat treatment at 90 °C (Fig. 5). Free PE started to degrade significantly after 2 h of heat treatment ($p < 0.05$), and only 56.7 ± 0.5% of PE remained after 24 h. Conversely, the retention rate of PE-NP after 24 h was 92.5 ± 1.3%. The retention rate of PE-NP after 24 h was significantly higher than that of free PE ($p < 0.05$).

These results were consistent with those of a previous study showing that heat treatment of free PE at 50, 80, and 100 °C reduced the DPPH radical scavenging effect, indicating that flavonoids in PE are highly unstable to heat (Lu, Chen, & Chou, 2003). In the previous study, the thermal stability of PE was enhanced by encapsulation within NP, confirmed by thermogravimetric analysis and differential thermal analysis (do Nascimento et al., 2022). Similarly, the retention rates of PE-NP were remarkably higher by 1.63-fold than free PE after 24 h of heat treatment. As confirmed by the differential scanning calorimetry thermogram, NP prepared with CS and HA protected the core material and weakened the effect of temperature owing to electrostatic interactions between CS and HA (Shabani Ravari et al., 2016). Considering the thermogravimetric analysis, the major decomposition of HA occurred between 200 and 300 °C with the breakage of the molecular structure and electrostatic property (Lewandowska, Sionkowska, Grabska, & Kaczmarek, 2016). Similarly, CS exhibited the main decomposition at temperature ranges of 210–240 °C (Woranuch & Yoksan, 2013). Therefore, heat treatment at 90 °C did not dramatically affect the structure and properties of CS and HA. In conclusion, the PE-NP prepared using CS and HA remarkably enhanced the thermal stability of PE.

3.4.2. Storage stability of the PE-NP

The retention rates and DPPH radical scavenging effects were monitored after storage at 30 and 50 °C for 4 weeks to investigate the storage stability of PE-NP. As shown in Fig. 6a and b, the retention rates

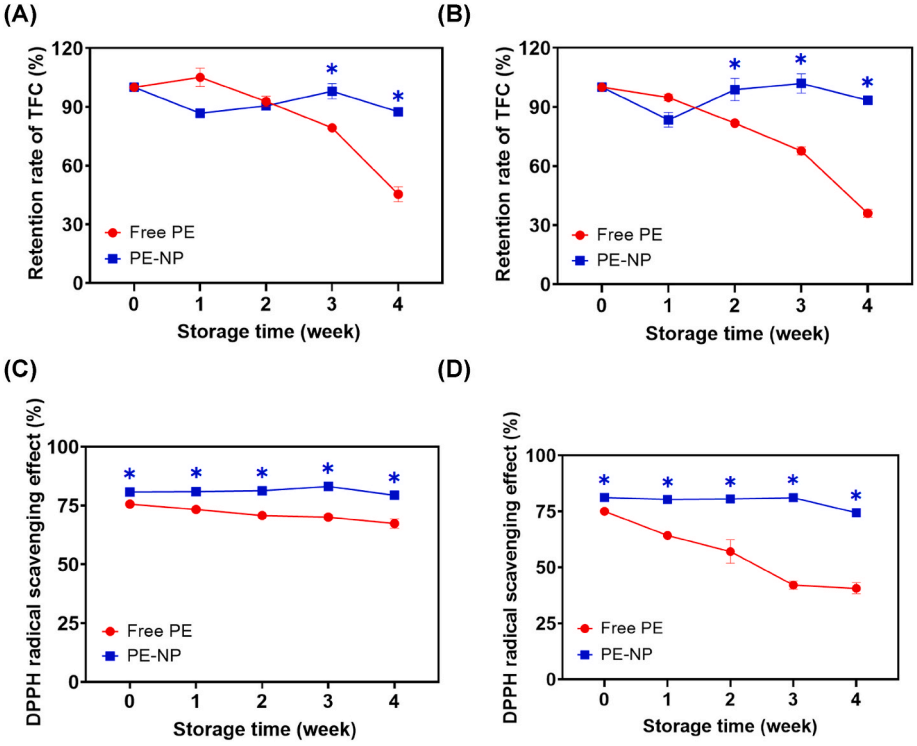

Fig. 6. The retention rate of TFC of free PE and PE-NP during their storage at (a) 30 and (b) 50 °C for 4 weeks. The DPPH radical scavenging effect of free PE and PE-NP during their storage at (c) 30 and (d) 50 °C. PE, propolis extract; PE-NP, propolis extract-loaded nanoparticles. All data are expressed as mean ± standard deviation. *Asterisk indicates a significant difference between the two groups using the Student's t-test at $p < 0.05$.

of TFC in free PE significantly decreased to 45.4 ± 3.8 and 36.1 ± 2.0% after storage at 30 and 50 °C, respectively ($p < 0.05$). In contrast, PE-NP exhibited significantly higher retention rates than free PE ($p < 0.05$). Furthermore, the DPPH radical scavenging effect of free PE significantly decreased to 40.6 ± 2.5 and 67.4 ± 2.0% at week 4 after storage at 30 and 50 °C, respectively, whereas PE-NP showed a constant antioxidant capacity during storage (Fig. 6c and d).

These results, which showed low storage stability of PE are consistent with previous findings that the stability of antioxidant activity of soft drinks containing PE ranged from 76.3 to 78.6% during 30 days of storage at 4, 25, and 45 °C (Vasilaki, Hatzikamari, Stagkos-Georgiadis, Goula, & Mourtzinos, 2019). To our knowledge, there is no study on the effects of enhancing the storage stability of PE-NP. In this study, PE-NP showed a smaller decrease in the retention rates of TFC than free PE. This may be related to the higher molecular weight of HA compared to that of other anionic biopolymers, resulting in a denser PE-NP structure (Akolade et al., 2017; Yang et al., 2015). Therefore, PE-NP may maintain their matrix throughout storage without structural degradation or the release of PE (Kim, Kim, Lee, & Lee, 2019). The increase in the DPPH radical scavenging effect after storage could be a result of the enhanced retention rate of TFC (Asem, Abdul Gapar, Abd Hapit, & Omar, 2020). Another reason for enhanced DPPH radical scavenging effect may be due to a higher initial DPPH radical scavenging effect than free PE. According to (Lee, Kim, & Lee, 2010; Luo et al., 2020), the increased antioxidant activity of PE-NP may be associated with their enhanced solubility, as described in Section 3.3. Similarly, our previous study reported that quercetin-loaded NP formulated with CS and HA had a higher DPPH radical scavenging effect than free quercetin (Kim et al., 2021). Collectively, these results suggest that PE-NP could be a potential method for improving the storage stability.

4. Conclusions

In the present study, we encapsulated PE within PE-NP via electrostatic interactions between CS and HA. Physicochemical characteristics, such as size, PDI, zeta potential, and entrapment efficiency were partially influenced by the ratios of CS to HA and core to wall. Considering PDI values lower than 0.3, a zeta potential higher than 20 mV, and entrapment efficiency, PE-NP with a 4:7 ratio of CS and HA and a 1:2 ratio of core and wall were found to be optimal. The solubility of free PE and PE-NP was 14.43 ± 0.71 and 35.03 ± 0.75 mg QUE/g, respectively, indicating that PE-NP showed a dramatic increase in solubility. Furthermore, the retention rate of TFC increased after encapsulation into PE-NP after both 24 h of heat treatment and 4 weeks of storage. In conclusion, PE-NP have great potential for enhancing solubility and thermal and storage stability. This research could provide helpful information for expanding the applications of PE in the food, pharmaceutical, and cosmetic industries.

Funding

This study was supported by the Korea Institute of Planning and Evaluation for Technology in Food, Agriculture, Forestry and Fisheries (IPET) through the High Value-added Food Technology Development Program, funded by the Ministry of Agriculture, Food and Rural Affairs (MAFRA) (121012-3).

CRediT authorship contribution statement

Do Hee Kim: Conceptualization, Data curation, Methodology, Formal analysis, Investigation, Validation, Writing – original draft, preparation. **Eun Woo Jeong:** Conceptualization, Investigation, Visualization, Writing – review & editing. **Youjin Baek:** Conceptualization, Writing – review & editing. **Hyeon Gyu Lee:** Conceptualization, Writing – review & editing, Project administration, Funding acquisition, Supervision.

Declaration of competing interest

The authors declare no conflict of interest.

Data availability

Data will be made available on request.

References

Akolade, J. O., Oloyede, H. O. B., & Onyenekwe, P. C. (2017). Encapsulation in chitosan-based polyelectrolyte complexes enhances antidiabetic activity of curcumin. *Journal of Functional Foods, 35*, 584–594. https://doi.org/10.1016/j.jff.2017.06.023

Anjum, S. I., Ullah, A., Khan, K. A., Attaullah, M., Khan, H., Ali, H., et al. (2019). Composition and functional properties of propolis (bee glue): A review. *Saudi Journal of Biological Sciences, 26*(7), 1695–1703. https://doi.org/10.1016/j.sjbs.2018.08.013

Anselmo, A. C., & Mitragotri, S. (2014). Cell-mediated delivery of nanoparticles: Taking advantage of circulatory cells to target nanoparticles. *Journal of Controlled Release, 190*, 531–541. https://doi.org/10.1016/j.jconrel.2014.03.050

Asem, N., Abdul Gapar, N. A., Abd Hapit, N. H., & Omar, E. A. (2020). Correlation between total phenolic and flavonoid contents with antioxidant activity of Malaysian stingless bee propolis extract. *Journal of Apicultural Research, 59*(4), 437–442. https://doi.org/10.1080/00218839.2019.1684050

Astutiningsih, F., Anggrahini, S., Fitriani, A., & Supriyadi, S. (2022). Optimization of saffron essential oil nanoparticles using chitosan-Arabic gum complex nanocarrier with ionic gelation method. International. *Journal of Food Science.* , Article 4035033. https://doi.org/10.1155/2022/4035033, 2022.

Bai, C., Zheng, J., Zhao, L., Chen, L., Xiong, H., & McClements, D. J. (2019). Development of oral delivery systems with enhanced antioxidant and anticancer activity: Coix seed oil and β-carotene coloaded liposomes. *Journal of Agricultural and Food Chemistry, 67*(1), 406–414. https://doi.org/10.1021/acs.jafc.8b04879

Boisard, S., Le Ray, A. M., Landreau, A., Kempf, M., Cassisa, V., Flurin, C., et al. (2015). Antifungal and antibacterial metabolites from a French poplar type propolis. *Evidence-based Complementary and Alternative Medicine.* , Article 319240. https://doi.org/10.1155/2015/319240, 2015.

Cavalu, S., Bisboaca, S., Mates, I. M., Pasca, P. M., Laslo, V., Costea, T., et al. (2018). Novel formulation based on chitosan-Arabic gum nanoparticles entrapping propolis extract. *Revista de Chimie, 69*, 3756–3760. https://doi.org/10.37358/RC.18.12.6836

Chang, X., Feng, W., He, L., Chen, X., & Liang, L. (2020). Fabrication and characterisation of whey protein isolate–propolis–alginate complex particles for stabilising α-tocopherol-contained emulsions. *International Dairy Journal, 109*, Article 104756. https://doi.org/10.1016/j.idairyj.2020.104756

Chang, C. C., Yang, M. H., Wen, H. M., & Chern, J. C. (2002). Estimation of total flavonoid content in propolis by two complementary colometric methods. *Journal of Food and Drug Analysis, 10*(3). https://doi.org/10.38212/2224-6614.2748. Article 3.

Chen, C., Chi, Y. J., & Xu, W. (2012). Comparisons on the functional properties and antioxidant activity of spray-dried and freeze-dried egg white protein hydrolysate. *Food and Bioprocess Technology, 5*(6), 2342–2352. https://doi.org/10.1007/s11947-011-0606-7

Choh, S. Y., Cross, D., & Wang, C. (2011). Facile synthesis and characterization of disulfide-cross-linked hyaluronic acid hydrogels for protein delivery and cell encapsulation. *Biomacromolecules, 12*(4), 1126–1136. https://doi.org/10.1021/bm101451k

Fang, Z., & Bhandari, B. (2010). Encapsulation of polyphenols–a review. *Trends in Food Science & Technology, 21*(10), 510–523. https://doi.org/10.1016/j.tifs.2010.08.003

Ghatak, D., & Iyyaswami, R. (2019). Selective encapsulation of quercetin from dry onion peel crude extract in reassembled casein particles. *Food and Bioproducts Processing, 115*, 100–109. https://doi.org/10.1016/j.fbp.2019.03.003

Iadnut, A., Mamoon, K., Thammasit, P., Pawichai, S., Tima, S., Preechasuth, K., et al. (2019). In vitro antifungal and antivirulence activities of biologically synthesized ethanolic extract of propolis-loaded PLGA nanoparticles against Candida albicans. *Evidence-based Complementary and Alternative Medicine.* , Article 3715481. https://doi.org/10.1155/2019/3715481, 2019.

Jansen-Alves, C., Krumreich, F. D., Zandoná, G. P., Gularte, M. A., Borges, C. D., & Zambiazi, R. C. (2019). Production of propolis extract microparticles with concentrated pea protein for application in food. *Food and Bioprocess Technology, 12*(5), 729–740. https://doi.org/10.1007/s11947-019-2246-2

Jeon, Y. O., Lee, J. S., & Lee, H. G. (2016). Improving solubility, stability, and cellular uptake of resveratrol by nanoencapsulation with chitosan and γ-poly (glutamic acid). *Colloids and Surfaces B: Biointerfaces, 147*, 224–233. https://doi.org/10.1016/j.colsurfb.2016.07.062

Kalogeropoulos, N., Konteles, S., Mourtzinos, I., Troullidou, E., Chiou, A., & Karathanos, V. T. (2009). Encapsulation of complex extracts in *β*-cyclodextrin: An application to propolis ethanolic extract. *Journal of Microencapsulation, 26*(7), 603–613. https://doi.org/10.3109/02652040802586373

Kaushik, V., & Roos, Y. H. (2007). Limonene encapsulation in freeze-drying of gum Arabic–sucrose–gelatin systems. *LWT - Food Science and Technology, 40*(8), 1381–1391. https://doi.org/10.1016/j.lwt.2006.10.008

Kim, E. S., Baek, Y., Yoo, H. J., Lee, J. S., & Lee, H. G. (2022). Chitosan-tripolyphosphate nanoparticles prepared by ionic gelation improve the antioxidant activities of astaxanthin in the in vitro and in vivo model. *Antioxidants, 11*(3), 479. https://doi.org/10.3390/antiox11030479

Kim, E. S., Kim, D. Y., Lee, J. S., & Lee, H. G. (2019). Mucoadhesive chitosan–gum Arabic nanoparticles enhance the absorption and antioxidant activity of quercetin in the intestinal cellular environment. *Journal of Agricultural and Food Chemistry, 67*(31), 8609–8616. https://doi.org/10.1021/acs.jafc.9b00008

Kim, E. S., Lee, J. S., & Lee, H. G. (2021). Quercetin delivery characteristics of chitosan nanoparticles prepared with different molecular weight polyanion cross-linkers. *Carbohydrate Polymers, 267*, Article 118157. https://doi.org/10.1016/j.carbpol.2021.118157

Lee, J. S., Kim, G. H., & Lee, H. G. (2010). Characteristics and antioxidant activity of Elsholtzia splendens extract-loaded nanoparticles. *Journal of Agricultural and Food Chemistry, 58*(6), 3316–3321. https://doi.org/10.1021/jf904091d

Lee, J. S., Kim, E. S., & Lee, H. G. (2017). Improving the water solubility and antimicrobial activity of silymarin by nanoencapsulation. *Colloids and Surfaces B: Biointerfaces, 154*, 171–177. https://doi.org/10.1016/j.colsurfb.2017.03.004

Lee, J. S., Suh, J. W., Kim, E. S., & Lee, H. G. (2017). Preparation and characterization of mucoadhesive nanoparticles for enhancing cellular uptake of coenzyme Q10. *Journal of Agricultural and Food Chemistry, 65*(40), 8930–8937. https://doi.org/10.1021/acs.jafc.7b03300

Lewandowska, K., Sionkowska, A., Grabska, S., & Kaczmarek, B. (2016). Surface and thermal properties of collagen/hyaluronic acid blends containing chitosan. *International Journal of Biological Macromolecules, 92*, 371–376. https://doi.org/10.1016/j.ijbiomac.2016.07.055

Li, R., Lin, D., Roos, Y. H., & Miao, S. (2019). Glass transition, structural relaxation and stability of spray-dried amorphous food solids: A review. *Drying Technology, 37*(3), 287–300. https://doi.org/10.1080/07373937.2018.1459680

Lu, L. C., Chen, Y. W., & Chou, C. C. (2003). Antibacterial and DPPH free radical-scavenging activities of the ethanol extract of propolis collected in Taiwan. *Journal of Food and Drug Analysis, 11*(4), 277–282. https://doi.org/10.38212/2224-6614.2676

Luo, M., Zhang, R., Liu, L., Chi, J., Huang, F., Dong, L., et al. (2020). Preparation, stability and antioxidant capacity of nano liposomes loaded with procyandins from lychee pericarp. *Journal of Food Engineering, 284*, Article 110065. https://doi.org/10.1016/j.jfoodeng.2020.110065

Lu, H. D., Zhao, H. Q., Wang, K., & Lv, L. L. (2011). Novel hyaluronic acid–chitosan nanoparticles as non-viral gene delivery vectors targeting osteoarthritis. *International Journal of Pharmaceutics, 420*(2), 358–365. https://doi.org/10.1016/j.ijpharm.2011.08.046

Muhammad, D. R. A., Doost, A. S., Gupta, V., bin Sintang, M. D., Van de Walle, D., Van der Meeren, P., et al. (2020). Stability and functionality of xanthan gum–shellac nanoparticles for the encapsulation of cinnamon bark extract. *Food Hydrocolloids, 100*, Article 105377. https://doi.org/10.1016/j.foodhyd.2019.105377

do Nascimento, T. G., de Almeida, C. P., da Conceição, M. M., dos Santos Silva, A., de Almeida, L. M., de Freitas, J. M. D., et al. (2022). Caseinates loaded with Brazilian red propolis extract: Preparation, protein-flavonoids interaction, antioxidant and antibacterial activities. *Journal of Thermal Analysis and Calorimetry, 147*(2), 1329–1343. https://doi.org/10.1007/s10973-020-10448-w

Oliveira, A. V., Bitoque, D. B., & Silva, G. A. (2014). Combining hyaluronic acid with chitosan enhances gene delivery. *Journal of Nanomaterials*. https://doi.org/10.1155/2014/246347, 2014. Article 152.

Oyarzun-Ampuero, F. A., Brea, J., Loza, M. I., Torres, D., & Alonso, M. J. (2009). Chitosan–hyaluronic acid nanoparticles loaded with heparin for the treatment of asthma. *International Journal of Pharmaceutics, 381*(2), 122–129. https://doi.org/10.1016/j.ijpharm.2009.04.009

Platt, V. M., & Szoka, F. C., Jr. (2008). Anticancer therapeutics: Targeting macromolecules and nanocarriers to hyaluronan or CD44, a hyaluronan receptor. *Molecular Pharmaceutics, 5*(4), 474–486. https://doi.org/10.1021/mp800024g

Ramli, N. A., Ali, N., Hamzah, S., & Yatim, N. I. (2021). Physicochemical characteristics of liposome encapsulation of stingless bees' propolis. *Heliyon, 7*(4), Article e06649. https://doi.org/10.1016/j.heliyon.2021.e06649

Santos, L. M., Fonseca, M. S., Sokolonski, A. R., Deegan, K. R., Araújo, R. P., Umsza-Guez, M. A., et al. (2020). Propolis: Types, composition, biological activities, and veterinary product patent prospecting. *Journal of the Science of Food and Agriculture, 100*(4), 1369–1382. https://doi.org/10.1002/jsfa.10024

Seibert, J. B., Bautista-Silva, J. P., Amparo, T. R., Petit, A., Pervier, P., dos Santos Almeida, J. C., et al. (2019). Development of propolis nanoemulsion with antioxidant and antimicrobial activity for use as a potential natural preservative. *Food Chemistry, 287*, 61–67. https://doi.org/10.1016/j.foodchem.2019.02.078

Shabani Ravari, N., Goodarzi, N., Alvandifar, F., Amini, M., Souri, E., Khoshayand, M. R., et al. (2016). Fabrication and biological evaluation of chitosan coated hyaluronic acid-docetaxel conjugate nanoparticles in CD44+ cancer cells. *Daru Journal of Pharmaceutical Sciences, 24*(1). https://doi.org/10.1186/s40199-016-0160-y. Article 21.

Shao, P., Xuan, S., Wu, W., & Qu, L. (2019). Encapsulation efficiency and controlled release of Ganoderma lucidum polysaccharide microcapsules by spray drying using different combinations of wall materials. *International Journal of Biological Macromolecules, 125*, 962–969. https://doi.org/10.1016/j.ijbiomac.2018.12.153

Smits, E. A., Smits, C. J., & Vromans, H. (2013). The development of a method to quantify encapsulated and free prednisolone phosphate in liposomal formulations. *Journal of Pharmaceutical and Biomedical Analysis, 75*, 47–54. https://doi.org/10.1016/j.jpba.2012.11.008

Vasilaki, A., Hatzikamari, M., Stagkos-Georgiadis, A., Goula, A. M., & Mourtzinos, I. (2019). A natural approach in food preservation: Propolis extract as sorbate alternative in non-carbonated beverage. *Food Chemistry, 298*, Article 125080. https://doi.org/10.1016/j.foodchem.2019.125080

Wei, W., Lu, M., Xu, W., Polyakov, N. E., Dushkin, A. V., & Su, W. K. (2022). Preparation of protamine-hyaluronic acid coated core-shell nanoparticles for enhanced solubility, permeability, and oral bioavailability of decoquinate. *International Journal of Biological Macromolecules, 218*, 346–355. https://doi.org/10.1016/j.ijbiomac.2022.07.152

Woranuch, S., & Yoksan, R. (2013). Eugenol-loaded chitosan nanoparticles: I. Thermal stability improvement of eugenol through encapsulation. *Carbohydrate Polymers, 96*(2), 578–585. https://doi.org/10.1016/j.carbpol.2012.08.117

Wu, Y., Yang, W., Wang, C., Hu, J., & Fu, S. (2005). Chitosan nanoparticles as a novel delivery system for ammonium glycyrrhizinate. *International Journal of Pharmaceutics, 295*(1–2), 235–245. https://doi.org/10.1016/j.ijpharm.2005.01.042

Yang, L., Gao, S., Asghar, S., Liu, G., Song, J., Wang, X., et al. (2015). Hyaluronic acid/chitosan nanoparticles for delivery of curcuminoid and its in vitro evaluation in glioma cells. *International Journal of Biological Macromolecules, 72*, 1391–1401. https://doi.org/10.1016/j.ijbiomac.2014.10.039

Yazicioglu, B., Sahin, S., & Sumnu, G. (2015). Microencapsulation of wheat germ oil. *Journal of Food Science and Technology, 52*(6), 3590–3597. https://doi.org/10.1007/s13197-014-1428-1

Zhang, H., Fu, Y., Niu, F., Li, Z., Ba, C., Jin, B., et al. (2018). Enhanced antioxidant activity and in vitro release of propolis by acid-induced aggregation using heat-denatured zein and carboxymethyl chitosan. *Food Hydrocolloids, 81*, 104–112. https://doi.org/10.1016/j.foodhyd.2018.02.019

Zhang, H., Fu, Y., Xu, Y., Niu, F., Li, Z., Ba, C., et al. (2019). One-step assembly of zein/caseinate/alginate nanoparticles for encapsulation and improved bioaccessibility of propolis. *Food & Function, 10*(2), 635–645. https://doi.org/10.1039/C8FO01614C